

## ARTICLE OPEN



# Vitamin E relieves chronic obstructive pulmonary disease by inhibiting COX2-mediated p-STAT3 nuclear translocation through the EGFR/MAPK signaling pathway

Hui Zhao<sup>1</sup>✉, Jiannan Gong<sup>1</sup>, Lifang Li<sup>1</sup>, Shuyin Zhi<sup>1</sup>, Guang Yang<sup>1</sup>, Pingping Li<sup>1</sup>, Ruina Li<sup>1</sup> and Jianqiang Li<sup>1</sup>

© The Author(s), under exclusive licence to United States and Canadian Academy of Pathology 2021

Patients with chronic obstructive pulmonary disease (COPD) are characterized by an imbalance between oxidant enzymes and antioxidant enzymes. In the present study, we explored the protective effect of vitamin E on COPD and the underlying mechanisms. Targets of vitamin E were predicted by bioinformatics analysis. After establishing cigarette smoke (CS)-induced COPD rats, the expression levels of epidermal growth factor receptor (EGFR), cyclooxygenase 2 (COX2), and transcriptional activity of signal transducer and activator of transcription 3 (STAT3) were measured. Additionally, the effects of vitamin E on CS-induced COPD were explored by assessing inflammation, the reactive oxygen species (ROS), the activity of superoxide dismutase (SOD) and the content of malondialdehyde (MDA), viability of human bronchial epithelioid (HBE) cells, and the expression of EGFR/MAPK pathway-related factors after loss- and gain- function assays. Vitamin E alleviated COPD. Vitamin E inhibited MAPK signaling pathway through decreasing EGFR expression. Additionally, vitamin E suppressed CS-induced HBE cell damage. Functionally, vitamin E attenuated CS-induced inflammation, apoptosis, and ROS by inhibiting the EGFR/MAPK axis, thereby inhibiting COX2-mediated p-STAT3 nuclear translocation. Moreover, overexpression of COX2 attenuated the protective effect of vitamin E on COPD rats. The present study shows that vitamin E inhibits the expression of COX2 by negatively regulating the EGFR/MAPK pathway, thereby inhibiting the translocation of phosphorylated STAT3 to the nucleus and relieving COPD.

*Laboratory Investigation* (2022) 102:272–280; <https://doi.org/10.1038/s41374-021-00652-z>

## INTRODUCTION

Chronic obstructive pulmonary disease (COPD) is a chronic and progressive disease with increasing prevalence and mortality, which poses a huge burden to the healthcare providers<sup>1</sup>. Patients with COPD show daily symptoms, including decreased ability to exercise that progressively gets worse, leading to a decline in health related quality of life<sup>2</sup>. It is characterized by chronic airflow obstruction and induced by an inflammatory response in the lung, mainly from cigarette smoke (CS)<sup>3</sup>, which stimulates the infiltration of lymphocytes and neutrophils to trigger the release of proinflammatory cytokines that contribute to tissue inflammation and remodeling<sup>4</sup>. Current treatment methods for COPD mainly include inhaler therapy, long-term oxygen therapy, smoking cessation with the aid of counseling and pharmacotherapy, pulmonary rehabilitation, and treatment of comorbidities<sup>5</sup>. However, in recent years, few advances have been made to ameliorate the progression of COPD or decrease its mortality, so a better understanding of the complex disease mechanisms resulting in COPD is needed<sup>6</sup>.

An imbalance between oxidants and antioxidants was shown to play a critical role in COPD pathogenesis<sup>7</sup>. Supplement of antioxidants like vitamin E in diet has potential to improve lung function<sup>8</sup>. It has been reported that  $\gamma$ -tocotrienol, a subtype of vitamin E, has both oxidative and antioxidant properties and prevents CS-induced emphysema in COPD<sup>9</sup>. Further, it is

documented that epidermal growth factor receptor (EGFR) and its downstream mitogen-activated protein kinase (MAPK) signaling pathway activities are increased in COPD<sup>10</sup>. Intriguingly, vitamin E can attenuate MAPK activation<sup>11</sup> and decrease the expression of EGFR<sup>12</sup>. Thus, we hypothesized that vitamin E may relieve COPD through the EGFR/MAPK pathway. Additionally, activation of MAPK can increase the expression of cyclooxygenase 2 (COX2)<sup>13</sup>. COX2 is an inducible enzyme regulated by NF- $\kappa$ B signaling and transcriptionally triggered by numerous stimuli<sup>14</sup> and plays a role in the nosogenesis of airway inflammation<sup>15</sup>. For example, curcumin reduces airway inflammation and remodeling through inhibiting NF- $\kappa$ B signaling and downregulating COX2 in mouse models induced by CS<sup>16</sup>. Thus, in the present study, the specific mechanisms of vitamin E in COPD by a possible EGFR/MAPK1/COX2 axis were studied, which may provide new insights into the potential therapeutic effects of vitamin E on COPD.

## MATERIALS AND METHODS

### Ethics statement

All animal experiments were approved by the Animal Care and Use Committee of The Second Hospital of Shanxi Medical University and in accordance with the guidance of National Institutes of Health. Great efforts were made to minimize the number of animals used in the experiments and their suffering.

<sup>1</sup>Department of Respiratory and Critical Care Medicine, The Second Hospital of Shanxi Medical University, Taiyuan 030001, PR China. ✉email: hui\_zhao@sxmu.edu.cn

Received: 23 February 2021 Revised: 21 July 2021 Accepted: 25 July 2021

Published online: 19 November 2021

## Bioinformatics analysis

Targets of vitamin E were predicted by the drug gene interaction database (DGIdb) (<http://dgidb.org/>). COPD-related genes were screened through the GeneCards database (<https://www.genecards.org/>) and the Comparative Toxicogenomics Database (CTD) (<http://ctdbase.org/>, score  $\geq 40$ ). Then, the overlapping parts of drugs and disease targets were found through the jvenn tool (<http://jvenn.toulouse.inra.fr/app/example.html>). By Network Analyst enrichment analysis tool (<https://www.networkanalyst.ca/>), we conducted KEGG enrichment analysis of candidate targets. Using the STRING tool (<https://string-db.org/>), the interacting regulators of the genes were predicted, and the gene interaction regulatory network was visualized using Cytoscape 3.5.1 software. Through the Coexpedia website (<http://www.coexpedia.org/>), the coexpression relationship between genes was analyzed. The Chipbase database (<http://rna.sysu.edu.cn/chipbase/>) was used to obtain the coexpression relationship between genes. Differential analysis of the COPD-related microarray dataset GSE3320 in the GEO database (<https://www.ncbi.nlm.nih.gov/gds>) was performed through the R language “limma” package (<http://www.bioconductor.org/packages/release/bioc/html/limma.html>) with  $|\log_2FC| \geq 0.55$ ,  $p \leq 0.05$  as the threshold value.

## Establishment and grouping of cigarette smoke (CS)-induced COPD rats

Sixty male Sprague-Dawley (SD) rats (180–200 g) were purchased from the animal experimental center of The Second Hospital of Shanxi Medical University and maintained at a constant ambient temperature ( $22 \pm 11^\circ\text{C}$ ) in a 12 h light–dark cycle. All rats were randomly divided into control group, CS group, CS + vitamin E group, vector + CS group, vector + CS + vitamin E group, and COX2 + CS + vitamin E group.

CS-induced COPD rats were constructed as follows. SD rats were placed in a 6 L plexiglass chamber and exposed to CS produced by 18 cigarettes for 40 min twice a day with a smoke-free interval of 6 h (6 days for a week). The unfiltered cigarettes used in this study contained 12 mg of tar and 1.25 mg of nicotine per cigarette (CHIENMEN; Shanghai Tobacco Factory, Shanghai, China). The rats in the control group were exposed to air on the same schedule for 12 weeks. For groups requiring vitamin E treatment, rats were fed 75 mg/kg vitamin E (S4686, Select Chemicals, and Houston, TX, USA) daily prior to CS treatment.

Adeno-associated virus (AAV6–COX2,  $1.5 \times 10^9/\text{mL}$ ) was purchased from Shanghai Menachem Co., Ltd. (Shanghai, China) and designed according to the rat Reeling sequence and synthesized by the company, and the experimental procedures were performed according to the instructions. For rats receiving only virus, rats were anesthetized by isoflurane inhalation. After confirming the depth of anesthesia, laryngoscopy was performed and the trachea was inserted with a 16-gauge intravenous catheter for installation of  $1 \times 10^9$  PFU of adeno-associated virus into the rats, and then the animals were extubated and allowed to recover from anesthesia.

## Pulmonary-function assessment

All rats were anesthetized with isoflurane inhalation. The trachea was opened with an inverted T-shaped incision over the upper trachea of the larynx close to the throat. Each animal was then placed in a forced lung-operating system connected to an animal lung-function tester (AniRes2005, Bestlab, Beijing China) to measure respiratory frequency (Hz), ratio of expiratory volume to vital capacity (FEV0.3/FVC), and peak expiratory flow (PEF) at 0.3 s.

## Hematoxylin–eosin (H&E) staining

The lower lobe of the right lung was removed, fixed in 4% paraformaldehyde, embedded in paraffin, cut into 4  $\mu\text{m}$ -thick sections, and stained with an H&E staining kit (C0105, Beyotime) according to the manufacturer's protocols. Briefly, the sections were treated with 70% ethanol for 10 s, 80% ethanol for 10 s, 90% ethanol for 10 s, and absolute ethanol for 10 s, and then cleared by xylene twice (each for 5 min). Finally, the sections were mounted and photographed under an inverted microscope (IX73, OLYMPUS Optical Co., Ltd, Tokyo, Japan).

## Immunohistochemical staining

The lower lobe of the right lung was removed, fixed in 4% paraformaldehyde, embedded in paraffin, and cut into 4  $\mu\text{m}$ -thick sections. The sections were then deparaffinized with xylene, rehydrated by gradient alcohol, and incubated with 3% hydrogen peroxide to block endogenous peroxidase

activity. Subsequently, the sections were boiled in 10 mM sodium citrate (pH 6.0) for 30 min, and then blocked in 10% normal goat serum for 15 min, followed by incubation with antibodies to EGFR (1:100, ab52894, Abcam, Cambridge, UK), COX2 (1:200, ab179800, Abcam) or signal transducer and activator of transcription 3 (STAT3) (1:200, ab68153, Abcam) overnight at  $4^\circ\text{C}$  in a humidified chamber. The next day, after PBS washes, the sections were incubated with biotinylated secondary antibody of goat anti-rabbit Immunoglobulin G (IgG; 1:500, ab6721, Abcam) for 20 min, and then incubated with horseradish peroxidase (HRP)–streptavidin reagent (Innova Biosciences, Cambridge, UK) for 20 min. Finally, immunoreactivity was detected with diaminobenzidine (DAB) kit (Invitrogen, Carlsbad, California, USA).

## Terminal deoxynucleotidyl transferase-mediated dUTP nick-end labeling (TUNEL) assay

Cell apoptosis in rat lung tissues was detected according to the instructions of TUNEL kit (C1098, Beyotime, Shanghai, China). In brief, paraffin sections of rat lung tissues were deparaffinized in xylene for 5–10 min, and deparaffinized in fresh xylene for another 5–10 min, followed by treatment with absolute ethanol for 5 min, 90% ethanol for 2 min, 80% ethanol for 2 min, 70% ethanol for 2 min, and distilled water for 2 min. Then, the sections were processed with 20  $\mu\text{g}/\text{mL}$  DNase-free proteinase K at  $20\text{--}37^\circ\text{C}$  for 15 min, washed three times with PBS, and incubated with 3%  $\text{H}_2\text{O}_2$  for 20 min at room temperature to inactivate endogenous peroxidase in the sections. After that, the sections were incubated with 50  $\mu\text{L}$  of TUNEL detection solution for 60 min, with 50  $\mu\text{L}$  of Streptavidin-HRP working solution for 30 min, and 0.2–0.5 mL of DAB solution for 5–30 min. Subsequently, the sections were mounted and photographed under an inverted microscope (IX73, OLYMPUS) with five different fields.

## Serum and bronchoalveolar lavage fluid (BALF) collection

Anesthesia was induced by isoflurane inhalation in all rats, and serum samples were obtained from the abdominal aorta and centrifuged at 3000 rpm for 10 min to collect the supernatant. Additionally, bronchoalveolar lavage was performed in the left lung after ligation of the right lung of rats in each group, and 3 mL of sterile PBS was instilled three times through the tracheal tube to collect the fluid (recovery above 80%) followed by centrifugation at  $4000 \times g$  for 10 min at  $4^\circ\text{C}$ . The supernatant was stored at  $-80^\circ\text{C}$  for subsequent inflammatory factor detection. After the precipitated cells were resuspended in 1 mL of sterile PBS, the total number of cells was counted by a hemocytometer, and 200 cells in BALF stained with Wright–Giemsa (C0131, Beyotime) were differentially identified under a light microscope. The total number of each cell type was determined by multiplying the percentage by the total number of cells.

## Measurement of STAT3 transcriptional activity

Nuclear protein was extracted from the lung tissue of rats in each group with a nuclear protein extraction kit (P0027, Beyotime), and then STAT3 transcriptional activity in the lung nuclear extract of rats in each group was detected according to a TransAM STAT3 transcription factor kit (45196, Activemotif, Carlsbad, California, USA).

## Cell transfection and CS extract preparation

Human bronchial epithelioid (HBE) cells were purchased from Procell (CL-0346, Procell, Wuhan, China) and cultured in DMEM medium (10569044, Gibco, Carlsbad, California, USA) containing 10% FBS (10099141, Gibco) and 1% penicillin–streptomycin (15070063, Gibco) at  $37^\circ\text{C}$  in a cell incubator with 5%  $\text{CO}_2$ . HBE cells were transfected with vector (over-expression control), EGFR, and COX2 using Lipofectamine 2000 (11668019, Invitrogen).

Cigarette extract was prepared as follows. Cigarettes were first placed at the midpoint of the desiccator, the smoke was pumped into a container containing 10 mL of PBS buffer, and then the vacuum-pump pressure was adjusted to ensure that the smoke dissolved into the PBS as much as possible. Next, the pH of CS solution was adjusted to 7.4, and a 0.22  $\mu\text{m}$  filter was used to filter and remove bacteria, particles, etc., in a super clean bench to attain 100% CS solution. Its content was measured by high-performance liquid chromatography using nicotine as a reference, and the content of nicotine in each prepared 100% CS solution was adjusted to be between 36  $\mu\text{g}/\text{mL}$  and 39  $\mu\text{g}/\text{mL}$ . Fresh CS solutions were prepared before each experiment and used within 24 h.

### Immunofluorescence

HBE cells were fixed in 4% paraformaldehyde and permeabilized with 0.1% Triton X-100, and sections were blocked with 10% normal donkey serum. Primary antibody of rabbit anti-STAT3 (ab68153, 1:200, Abcam) was added and incubated overnight at 4 °C. The next day, sections were washed with PBS, and then probed with secondary antibody of Alexa Fluor488-conjugated goat anti-rabbit IgG (ab150077, 1:200, Abcam) for 1 h at room temperature. After washing with PBS, the sections were mounted with DAPI mounting medium (C1006, Beyotime) and photographed under a fluorescence microscope (BX63, Olympus, Tokyo, Japan).

### Cell counting kit-8 (CCK-8) assay

Cell proliferation was detected with CCK-8 kit (WH1199, Shanghai Biotechwell Co., Ltd., Shanghai, China). Briefly, cells in logarithmic growth phase were adjusted to a concentration of  $5 \times 10^4$  cells/mL and spread into a 96-well culture plate followed by addition of 100  $\mu$ L of cell culture medium into each well and culture for 48 h. The supernatant was quickly discarded, and 10  $\mu$ L of CCK-8 solution was added to each well. After 2 h of culture at 37 °C, the absorbance value (A) was measured with a Multiskan FC microplate reader (51119080, Thermo Fisher Scientific, USA) at a wavelength of 450 nm. The proliferation rate (%) =  $[(A_{\text{control group}} - A_{\text{experimental group}}) / A_{\text{control group}}] \times 100\%$ .

### Flow cytometry

Apoptosis of HBE cells was detected by AnnexinV-fluorescein isothiocyanate (FITC)/propidium iodide (PI) double staining. Cells were seeded in 6-well plates at  $2 \times 10^5$  cells/well, washed once with precooled PBS at 4 °C, detached with trypsin, and collected in a 15 mL centrifuge tube followed by centrifugation at 800 g to discard the supernatant. After washing and precipitating twice with PBS, the cells were resuspended in 500  $\mu$ L of binding buffer according to the instructions of the Apoptosis Detection Kit (556547, BD Bioscience, USA), added with 5  $\mu$ L of FITC and 5  $\mu$ L of PI in the dark and mixed well, and incubated for 15 min. Finally, apoptosis was detected by flow cytometry (BD FACSCalibur).

### Reverse-transcription quantitative polymerase chain reaction (RT-qPCR)

Total RNA was extracted from tissues using Trizol (16096020, Invitrogen, USA), and was reversely transcribed into complementary DNA (cDNA) using a reverse transcription kit (RR047A, Takara, Tokyo, Japan).

RT-qPCR was performed according to TaqMan Gene Expression Assays protocol (Applied Biosystems, Foster City, CA, USA). Primers were designed based on National Center of Biotechnology Information (NCBI) (<https://www.ncbi.nlm.nih.gov/tools/primer-blast/>) with the sequence shown in Supplementary Table 1. The relative transcriptional level of the gene to be tested was calculated by  $2^{-\Delta\Delta CT}$  method. Rat stands for rat and H for human.

### Western blot analysis

Radio-immunoprecipitation assay (RIPA) lysis solution (Beyotime Biotechnology, Shanghai, China) was used to extract total protein from cells in each group, and bicinchoninic acid (BCA) kit (20201E576, Yeasen Biotechnology Co. Ltd., Shanghai, China) was used to determine protein concentration. Quantification was performed according to different concentrations, and proteins were separated by polyacrylamide gel electrophoresis and transferred onto a polyvinylidene fluoride membrane (IPVH85R, Millipore, Germany) using the wet-transfer method and blocked with 5% BSA for 1 h at room temperature. Then the membrane was probed with primary antibodies against COX2 (1: 1000, ab179800, Abcam), EGFR (1:2000, ab52894, Abcam), STAT3 (1:1000, ab68153, Abcam), p-STAT3 (1:1000, ab76315, Abcam), p38 (1:1000, 9212, Cell Signaling Technologies [CST], Beverly, MA, USA), p-p38 (1:1000, 9211, CST), JNK (1:2000, 9252, CST), p-JNK (1:2000, 9255, CST), ERK1/2 (1:1000, 4695, CST), p-ERK1/2 (1:1000, 4370, CST), and GAPDH (1:5000, ab8254, Abcam) overnight at 4 °C. After three Tris-Buffered Saline Tween-20 (TBST) washes, the membrane was reprobed with HRP-labeled goat anti-rabbit IgG (ab6721, Abcam) or goat anti-mouse IgG (ab6789, Abcam) for 1 h at room temperature. Following TBST washes, luminescent solution was added for developing images. ImageJ software (National Institutes of Health) was used for protein quantitative analysis with  $\beta$ -actin as the internal reference.

### Reactive oxygen species (ROS) measurement

ROS in rat lung tissues were detected by DHE (S0063, Beyotime) staining. Lung tissues were selected for cryotomy and then incubated with 4  $\mu$ M DHE for 1 h at 37 °C in the dark and washed twice with PBS. Five different fields were selected for observation and photography under a FV-1000/ES confocal microscope, and the sections were quantified by ImageJ software. For HBE cells, ROS assay kit (S0033, Beyotime) was used for detection by flow cytometry.

### Detection of malondialdehyde (MDA) and superoxide dismutase (SOD) activity

Commercial kits were used for the detection of SOD activity and MDA content in rat lung tissues and HBE cells according to the instructions. Superoxide Dismutase Activity Assay Kit (ab65354, Abcam) was used for SOD activity assay and Lipid Peroxidation (MDA) Assay Kit (ab233471, Abcam) for measuring MDA content.

### Enzyme-linked immunosorbent assay (ELISA)

The contents of IL-1 $\beta$  (PI305, Beyotime, Shanghai, China), TNF- $\alpha$  (PT518, Beyotime) and IL-6 (PI330, Beyotime) were determined in the supernatant of HBE cells with ELISA kits, and those in the rat BALF were determined using IL-1 $\beta$  (PI303, Beyotime, China), TNF- $\alpha$  (PT516, Beyotime, China) and IL-6 (PI328, Beyotime, China) ELISA kits, based on the manufacturers' instructions. The experiment was repeated 3 times.

### Statistical analysis

GraphPad Prism software was used for statistical analysis, and *p* values were determined by performing a two-tailed *t*-test on independent samples. Measurement data were expressed as the mean  $\pm$  standard deviation. The comparison between two groups was conducted by independent-sample *t*-test. The comparison between multiple groups was performed by one-way analysis of variance (ANOVA) and Tukey's post hoc test. A value of *p* < 0.05 was considered a significant difference.

## RESULTS

### Vitamin E alleviates COPD

To explore the effect of vitamin E on COPD, we constructed rat COPD models. Compared with the normal rats, the COPD rats showed reduced body weight, increased respiratory frequency (Hz), and decreased PEF and FEV<sub>0.3</sub>/FVC, while the above results were reversed after vitamin E treatment (Fig. 1A, B). The results of H&E staining in the lungs of control rats showed the bronchial mucosal epithelium and alveolar structure in the lung tissues were intact, and no significant inflammatory cell infiltration was observed in the submucosa. While for the CS-treated rats, the bronchial epithelial cells in the lung tissues were disorganized, accompanied by a large number of inflammatory cell infiltration and a large number of inflammatory cell infiltration was observed in the pulmonary interstitium and alveolar space. In the CS-treated rats, treatment of vitamin E alleviated the bronchial wall thickening in the lung tissue, increased the number of alveoli, and reduced the inflammatory cell infiltration in the lung tissue (Fig. 1C). The results of TUNEL assay showed that the apoptosis rate in the lungs of rats was increased after CS treatment, but the elevated apoptosis rate in the CS-treated rats was recovered by vitamin E treatment (Fig. 1D). The counting of inflammatory cells in BALF revealed that the number of total inflammatory cells, neutrophils, macrophages, and lymphocytes was increased in BALF of the COPD rats, but the number of those cells was decreased after vitamin E treatment (Fig. 1E). In addition, the expression levels of inflammatory cytokines IL-1 $\beta$ , TNF- $\alpha$ , and IL-6 in the serum and BALF of rats in the COPD rats were significantly enhanced, while vitamin E treatment led to the opposite effects (Fig. 1F, G). Our findings unravelled that CS significantly increased the DHE fluorescence intensity, upregulated MDA content, and reduced SOD content in the rat lung tissues, while vitamin E resulted in the opposite trends (Fig. 1H, I). In a word, vitamin E

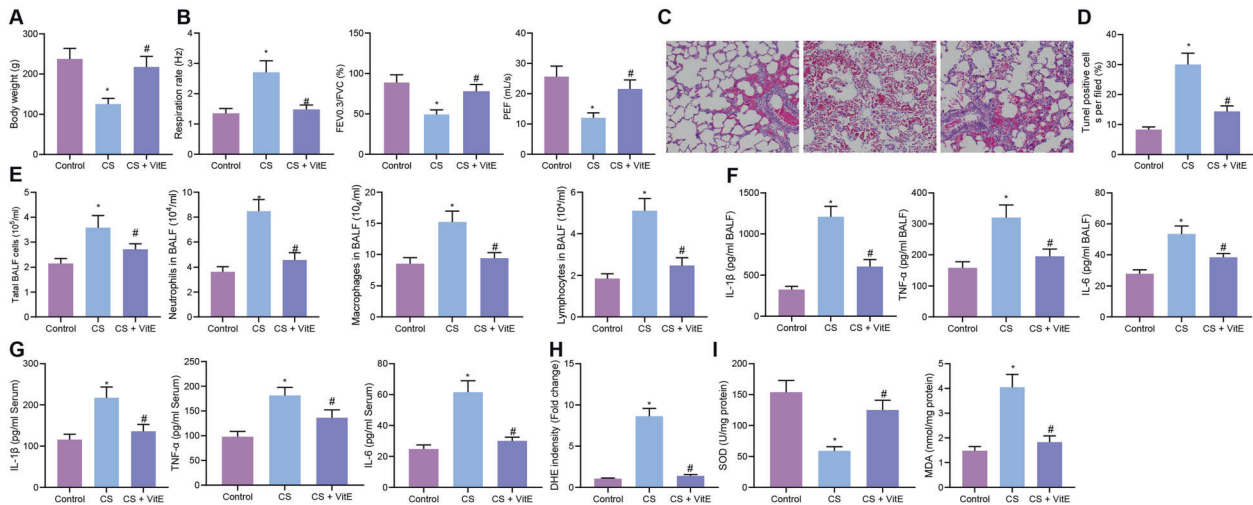


**Fig. 1** Vitamin E attenuates apoptosis, inflammation, and ROS production in the lungs of COPD rats. **A** Statistical map of body weight of rats after CS or vitamin E treatment. **B** Respiratory frequency (Hz), FEV0.3/FVC, and PEF at 0.3 s in rats after CS or vitamin E treatment. **C** H&E staining images of lung tissue sections of rats after CS or vitamin E treatment, wherein red arrow is inflammatory cell infiltration area and black arrow is alveolar space. **D** TUNEL staining of lung tissue sections of rats after CS or vitamin E treatment. **E** The number of total inflammatory cells, neutrophils, macrophages, and lymphocytes in BALF of rats after CS or vitamin E treatment. **F** ELISA was used to measure the expression of inflammatory cytokines IL-1 $\beta$ , TNF- $\alpha$ , and IL-6 in BALF of rats after CS or vitamin E treatment. **G** ELISA was employed to measure the expression of inflammatory cytokines IL-1 $\beta$ , TNF- $\alpha$ , and IL-6 in serum of rats after CS or vitamin E treatment. **H** DHE staining was used to detect ROS in lung tissue sections of rats after CS or vitamin E treatment. **I** The SOD activity and MDA content in lung tissues of rats after CS or vitamin E treatment. The data in the figure are measurement data and are expressed by the mean  $\pm$  standard deviation. The data in each group are analyzed by unpaired *t*-test, and the comparison among multiple groups is performed by one-way ANOVA and Tukey's post hoc test. \**p* < 0.05 vs. the control group, #*p* < 0.05 vs. the CS group, *n* = 6.

inhibited apoptosis, inflammation, and ROS production in the lungs of COPD rats.

### Vitamin E decreases EGFR expression and inhibits the MAPK signaling pathway

To explore the downstream regulatory mechanism of vitamin E in COPD, we first predicted 34 vitamin E targets through the DGIdb database and then obtained 6060 COPD-related genes through the GeneCards database. After intersection, 30 candidate genes were obtained, and a network diagram of gene-drug-disease interactions was drawn (Fig. 2A, B). The results of Network Analyst enrichment analysis showed that the candidate genes were mainly involved in EGFR/MAPK signaling pathways (Fig. 2C). Therefore, we speculated that vitamin E may inhibit MAPK signaling pathway by decreasing EGFR expression. To test this conjecture, we found that EGFR was highly expressed in COPD samples by analyzing the COPD-related microarray dataset GSE3320 in the GEO database (Fig. 2D). Immunohistochemical results and Western blot analysis revealed that EGFR expression as well as the total expression of MAPK pathway-related proteins ERK1/2, JNK, and p38 and the corresponding phosphorylated protein ratio in the lungs of CS-treated rats were increased, while vitamin E led to the opposite trends (Fig. 2E–G). Taken together, vitamin E decreased EGFR expression and inactivated MAPK signaling pathway.

### Vitamin E suppresses CS-induced HBE cell damage

To investigate the effect of vitamin E on CS-induced damage in HBE cells by regulating the EGFR/MAPK axis, we first validated by RT-qPCR that transfection with plasmid-overexpressing EGFR increased EGFR expression in HBE cells (Fig. 3A). Next, Western blot results showed that the expression of ERK1/2, JNK, and p38 and the corresponding phosphorylated protein ratio were significantly increased in the vector + CS group compared with the Vector group and increased in the EGFR + CS + vitamin E group compared with the vector + CS + vitamin E group. While the expression of ERK1/2, JNK, and p38 and the corresponding phosphorylated protein ratio was significantly decreased in the vector + CS +

vitamin E group compared with the vector + CS group (Fig. 3B, C). The results of CCK8 assay and Annexin V/PI staining showed that the cell viability decreased and apoptosis increased in the vector + CS group compared with the vector group, and also in the EGFR + CS + vitamin E group compared with the vector + CS + vitamin E group, while the cell viability increased and apoptosis reduced in the vector + CS + vitamin E group compared with the vector + CS group (Fig. 3D, E). Further, ELISA results showed that the contents of inflammatory factors in the cell supernatant of the vector + CS group increased compared with the vector group and also in the EGFR + CS + vitamin E group compared with the vector + CS + vitamin E group, while the contents of inflammatory factors in the cell supernatant of the vector + CS + vitamin E group reduced compared with the vector + CS group (Fig. 3F). In addition, we also found that ROS and MDA contents increased and SOD activity decreased in the vector + CS group compared with the Vector group and also in the EGFR + CS + vitamin E group compared with the vector + CS + vitamin E group, while ROS and MDA contents decreased and SOD activity increased in the vector + CS + vitamin E group compared with the vector + CS group (Fig. 3G, H). Taken together, vitamin E negatively regulated the MAPK pathway by inhibiting EGFR expression, thereby inhibiting CS-induced apoptosis, inflammation, and ROS production.

### Vitamin E inhibits COX2-mediated STAT3 nuclear entry by negatively regulating the EGFR/MAPK pathway

To explore the downstream regulatory mechanism of EGFR/MAPK pathway, we predicted 823 MAPK1-interacting genes by GeneCards database, 176 COPD-related genes by CTD database, and then intersected them to obtain 36 candidate genes (Fig. 4A). Analysis of the Coexpedia website suggested a coexpression relationship among the 36 candidate genes, with a high prediction score (score > 20) for the coexpression relationship of FOS, DUSP1, EGFR1, ATF3, VIM, PECAM1, ITGB2, VCAM1, and PTGS2 (Alias: COX-2) found (Fig. 4B). RT-qPCR results showed that CS increased the COX2 mRNA expression, while vitamin E decreased the COX2 mRNA expression on this basis (Fig. 4C).

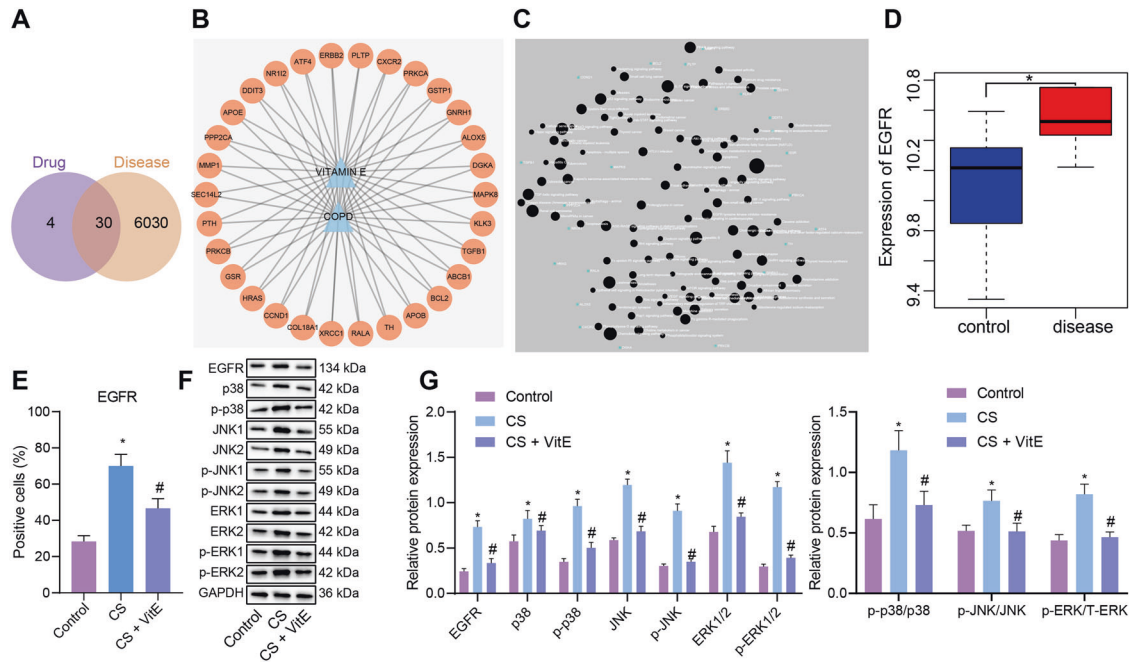


**Fig. 2** Vitamin E downregulates EGFR and inactivates MAPK signaling pathway. **A** Venn diagram of the intersection of drug and disease targets. **B** Network diagram of gene-drug-disease interaction relationship. **C** KEGG enrichment analysis results of 30 candidate targets. **D** Box diagram of EGFR expression in COPD attained through microarray dataset GSE3320, wherein blue box on the left indicates normal tissue samples and red box on the right indicates COPD samples. **E** EGFR expression in lung tissues of rats after CS or vitamin E treatment was detected by immunohistochemistry. **F** EGFR, p38, p-p38, JNK, p-JNK, ERK1/2, and p-ERK1/2 protein expression in lung tissues of rats after CS or vitamin E treatment was detected by Western blot. **G** Statistical diagram of Panel F. The data of each group are analyzed by unpaired *t*-test, and the data among multiple groups are compared by one-way ANOVA and Tukey's post hoc test. \**p* < 0.05 vs. the control group, #*p* < 0.05 vs. the CS group, *n* = 6.

Immunohistochemical results revealed that COX2 and STAT3 were highly expressed after CS treatment, while their expression was reduced by the further treatment of vitamin E (Fig. 4D). Further, we found that CS increased STAT3 transcriptional activity, while vitamin E decreased the transcriptional activity of STAT3 (Fig. 4E). These results indicated that vitamin E inhibited COX2 expression and nuclear entry of STAT3. To investigate whether vitamin E suppresses COX2-mediated STAT3 nuclear entry by negatively regulating the EGFR/MAPK pathway, plasmid-overexpressing EGFR was transfected in HBE cells, and the effect was verified by RT-qPCR (Fig. 4F). Next, Western blot results showed increased proportion of COX2 and STAT3 phosphorylation in the vector + CS group compared with the Vector group, and in the EGFR + CS + vitamin E and COX2 + CS + vitamin E groups compared with the vector + CS + vitamin E group, but the proportion of COX2 and STAT3 phosphorylation was reduced in the vector + CS + vitamin E group compared with the vector + CS group (Fig. 4G). Immunofluorescence results uncovered that STAT3 nuclear localization was significantly increased in the vector + CS group compared with the Vector group, and also in the EGFR + CS + vitamin E and COX2 + CS + vitamin E groups compared with the vector + CS + vitamin E group; STAT3 nuclear localization was reduced in the vector + CS + vitamin E group compared with the vector + CS group (Fig. 4H). Taken together, vitamin E inhibits COX2-mediated STAT3 nuclear entry by negatively regulating the EGFR/MAPK pathway.

### Vitamin E alleviates COPD by inhibiting STAT3 phosphorylation into the nucleus via the EGFR/MAPK1/COX2 pathway

To further verify that vitamin E inhibits STAT3 phosphorylation through the EGFR/MAPK1/COX2 pathway to ameliorate COPD in vivo, we measured COX2, STAT3, and p-STAT3 expression levels

in the lung tissues of COPD rat models with different treatments by Western blot. The results showed that the phosphorylation ratio of COX2 and STAT3 was significantly decreased in the vector + CS + vitamin E group compared with the vector + CS group, while the phosphorylation ratio of COX2 and STAT3 was significantly increased in the COX2 + CS + vitamin E group compared with the vector + CS + vitamin E group (Fig. 5A). Immunohistochemical results showed that STAT3 expression was lower and nuclear expression of STAT3 was decreased in the vector + CS + vitamin E group compared with the vector + CS group, while STAT3 was unchanged but nuclear expression of STAT3 was increased in the COX2 + CS + vitamin E group compared with the vector + CS + vitamin E group (Fig. 5B). Rats in the vector + CS + vitamin E group had significantly increased body weight, decreased respiratory frequency (Hz), and increased values of PEF and FEV0.3/FVC compared with the vector + CS group. While rats in the COX2 + CS + vitamin E group had significantly decreased body weight, increased respiratory frequency (Hz), and decreased values of PEF and FEV0.3/FVC compared with the vector + CS + vitamin E group (Fig. 5C, D). The results of H&E staining in the lungs of rats uncovered that the bronchial wall was thickened, the number of alveoli was significantly reduced, and the infiltration of inflammatory cells in the lung tissue was increased in the COX2 + CS + vitamin E group compared with the vector + CS + vitamin E group; the bronchial wall thickening in the lung tissue was alleviated, the number of alveoli was significantly increased, and the infiltration of inflammatory cells in the lung tissue was decreased in the vector + CS + vitamin E group compared with the vector + CS group (Fig. 5E). After TUNEL assay and measurements of inflammatory cell count in BALF of rats, we found that the apoptosis rate, the number of total inflammatory cells, neutrophils, macrophages, and lymphocytes in BALF was significantly reduced in the vector + CS + vitamin E group compared with the vector + CS group, while the apoptosis rate, the number of total inflammatory cells, neutrophils,

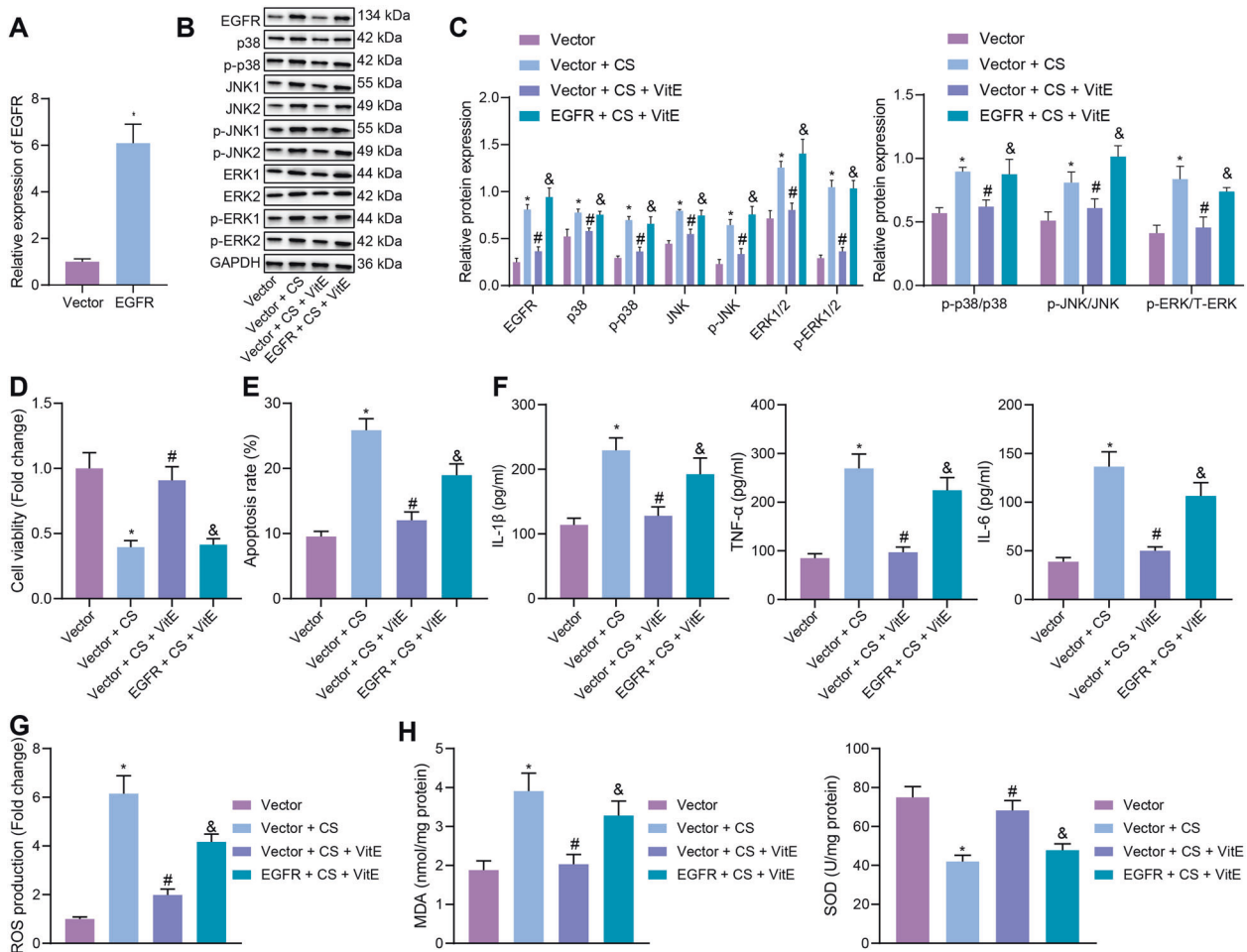


**Fig. 3** Vitamin E relieves CS-induced HBE cell damage. **A** RT-qPCR was used to assess the expression of EGFR in HBE cells of each group. **B** Western blot was used to assess the expression of EGFR, p38, p-p38, JNK, p-JNK, ERK1/2, and p-ERK1/2 in HBE cells of each group. **C** Statistical map of Panel B. **D** CCK8 assay was used to detect the viability of HBE cells in each group. **E** Annexin V/PI staining was used to detect the apoptosis of HBE cells in each group. **F** ELISA was used to detect the expression of inflammatory factors in the supernatant of HBE cells of each group. **G** ROS level in HBE cells of each group. **H** The SOD activity and MDA content in HBE cells of each group. The data in the figure were all measurement data, expressed as the mean  $\pm$  standard deviation. The data of each group were analyzed by unpaired *t*-test, and the comparison of data among multiple groups was performed by one-way ANOVA and Tukey's post hoc test. \**p* < 0.05 vs. the Vector group, #*p* < 0.05 vs. the vector + CS group, and &*p* < 0.05 vs. the vector + CS + vitamin E group.

macrophages, and lymphocytes in BALF was significantly increased in the lungs of rats in the COX2 + CS + vitamin E group compared with the vector + CS + vitamin E group (Fig. 5F, G). In addition, the expression levels of IL-1 $\beta$ , TNF- $\alpha$ , and IL-6 in serum and BALF, as well as the DHE fluorescence intensity were significantly reduced in the vector + CS + vitamin E group compared with the vector + CS group; however, they were increased in the COX2 + CS + vitamin E group compared with the vector + CS + vitamin E group (Fig. 5H–J). Moreover, we also observed that SOD activity increased, and MDA content decreased significantly in the vector + CS + vitamin E group compared with the vector + CS group, while SOD activity decreased and MDA content increased significantly in the COX2 + CS + vitamin E group compared with the vector + CS + vitamin E group (Fig. 5K). Altogether, vitamin E inhibited STAT3 phosphorylation into the nucleus through the EGFR/MAPK1/COX2 pathway to inhibit apoptosis, inflammation, and ROS production in the lungs of COPD rats.

## DISCUSSION

The definition of COPD is persistent airflow obstruction owing to chronic inflammation in the lung and the airways induced by

noxious stimuli. Existing therapies have not remarkably reduced the mortality of COPD patients<sup>3</sup>. To provide new basis for developing more effective drugs to treat this disease, we demonstrated the protective effect of vitamin E on COPD. We found that vitamin E improves COPD by blocking the EGFR/MAPK pathway and further suppressing COX2-mediated translocation of phosphorylated STAT3 to the nucleus (Fig. 6).

We determined that vitamin E relieved COPD. It has been shown that in some patients, COPD may result from oxidative stress caused by a lack of antioxidant nutrients<sup>17</sup>. It has been reported that vitamin E plays a beneficial role in relieving respiratory conditions of various origins by regulation of surfactant functions both in humans and animals<sup>18</sup>. A previous study found that vitamin E in lung tissues of patients with COPD was associated with disease severity<sup>19</sup>, which is consistent with our finding. Also, it has been observed that compared with healthy individuals, subjects with COPD consumed lower levels of antioxidants, especially vitamin C and vitamin E<sup>20,21</sup>.

Mechanistically, vitamin E suppressed COX2-mediated translocation of phosphorylated STAT3 to the nucleus through inhibition of the EGFR/MAPK signaling pathway, thereby alleviating COPD. Previous research has indicated that HIF-1 $\alpha$  has a promotive effect

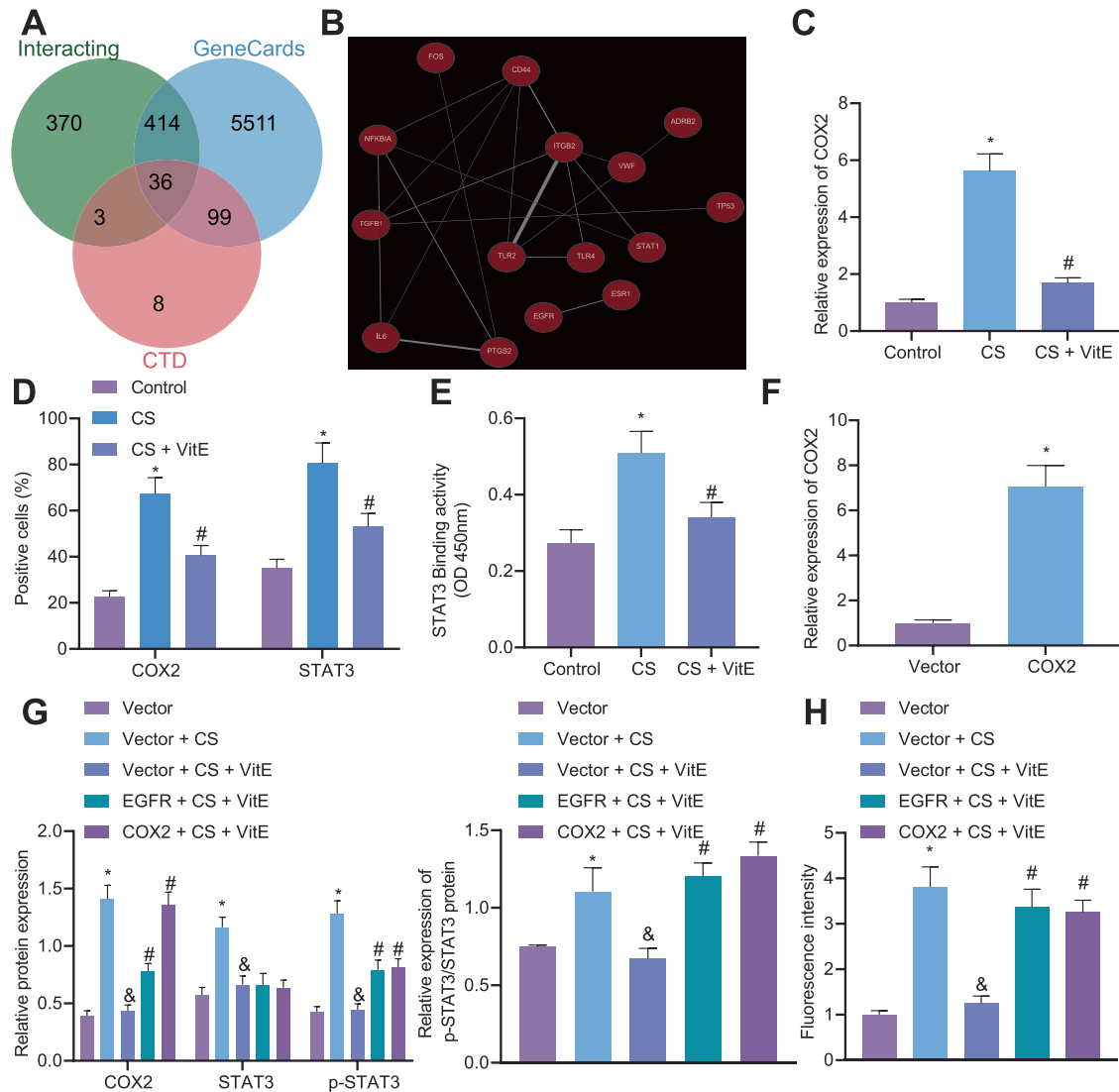


**Fig. 4** Vitamin E negatively regulates the EGFR/MAPK pathway to inhibit COX2-mediated STAT3 nuclear entry. **A** Venn diagram displaying the intersection of MAPK-interacting genes with disease-related genes in GeneCards and CTD database. **B** The coexpression relationship between 36 candidate genes attained through coexpedia website. **C** RT-qPCR to detect the expression of COX2 in the lung tissues of rats after CS or vitamin E treatment. **D** Immunohistochemistry to measure the expression of COX2 and STAT3 in the lung tissues of rats after CS or vitamin E treatment. **E** The transcriptional activity of STAT3 in the nuclear extract of lung tissues of rats after CS or vitamin E treatment. **F** RT-qPCR to detect the expression of COX2 in HBE cells in each group. **G** Western blot to detect the expression of COX2 and STAT3/p-STAT3 in HBE cells in each group. **H** Immunofluorescence to detect the localization of STAT3 in HBE cells in each group. The data in the figure were all measurement data, expressed as the mean  $\pm$  standard deviation. The data of each group were analyzed by unpaired *t*-test, and the comparison of data among multiple groups was performed by one-way ANOVA and Tukey's post hoc test. In animal tests, \**p* < 0.05 vs. the control group, and #*p* < 0.05 vs. the CS group. In cell experiments, \**p* < 0.05 vs. the Vector group, and #*p* < 0.05 vs. the vector + CS + vitamin E group.

on the inflammatory response of COPD by activation of the EGFR/PI3K/AKT signaling pathway<sup>22</sup>, and reducing the activity of EGFR could serve as a therapeutic strategy for relieving the inflammation and tissue remodeling observed in patients with COPD<sup>23</sup>. MAPK can be activated by a variety of stress stimuli, including TNF- $\alpha$  and ROS, and suppression of MAPK pathway has a substantial effect on ameliorating airway remodeling<sup>24,25</sup>. Further, it is noteworthy that the activities of EGFR and its downstream MAPK signaling pathway are both activated in COPD<sup>10</sup>. Interestingly, vitamin E has been reported to attenuate EGFR-AKT-STAT3 pathway<sup>12</sup> and to inactivate MAPK signaling<sup>11</sup>. From above, the inhibitive role of vitamin E on EGFR/MAPK pathway has been verified. Furthermore, the expression of COX2 can be elevated by activation of MAPK signaling pathway<sup>26</sup>. COX2 has been implicated in the nosogenesis of airway inflammation<sup>15</sup>,

implying its contributive effect on COPD. Another report has also suggested that down regulation of COX2 and inhibition of NF- $\kappa$ B signaling pathway could alleviate airway inflammation and airway remodeling in CS-induced COPD mouse models<sup>16</sup>. In addition, knockdown of COX2 inhibits the Tyr705 phosphorylation of STAT3, a site modification that is critical for oxidative stress<sup>27</sup>. STAT3 is a multifaceted oncoprotein that modulates immunity and inflammation, and is known as a tyrosine-phosphorylated transcription factor that regulates the expression of numerous genes<sup>28,29</sup>. Importantly, aerobic exercise reduces CS-induced COPD phenotype by down-regulation of CS-induced STAT3 and p-STAT3 in peribronchial leukocytes, airway epithelial cells, and parenchymal leukocytes<sup>30</sup>.

In summary, this paper reveals a new role for the antioxidant vitamin E in the regulation of COPD, suppression of the EGFR/

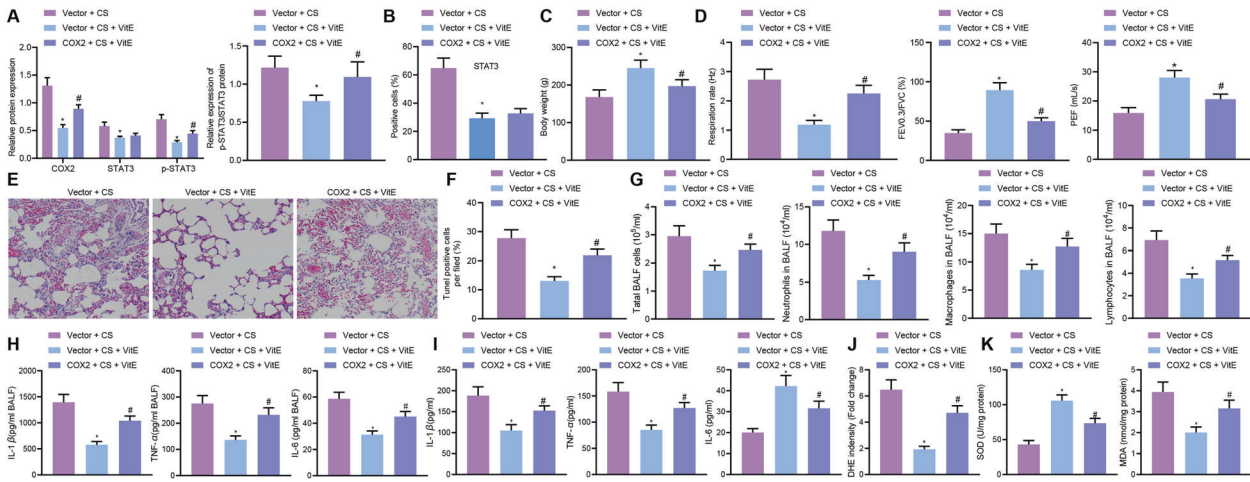


**Fig. 5 Vitamin E inhibits apoptosis, inflammation, and ROS production in the lungs of COPD rats through EGFR/MAPK1/COX2/STAT3 axis.** **A** Western blot was used to detect the expression of COX2 and STAT3/p-STAT3 in the lung tissues of rats in each group. **B** Immunohistochemistry was used to detect the expression of STAT3 in the lung tissues of rats in each group. **C** Statistical map of body weight of rats in each group. **D** The Hz, FEV0.3/FVC, and PEF of rats in each group at 0.3 s. **E** H&E staining map of lung tissue sections of rats in each group. **F** TUNEL staining of lung tissue sections of rats in each group. **G** The number of total inflammatory cells, neutrophils, macrophages, and lymphocytes in BALF of rats in each group. **H** ELISA was used to detect the expression of inflammatory cytokines IL-1 $\beta$ , TNF- $\alpha$ , and IL-6 in BALF of rats in each group. **I** ELISA was applied to detect the expression of inflammatory cytokines IL-1 $\beta$ , TNF- $\alpha$ , and IL-6 in serum of rats in each group. **J** DHE staining was adopted to detect ROS in lung tissue sections of rats in each group. **K** The SOD activity and MDA content in lung tissues of rats in each group. The data in the figure were all measurement data, expressed as the mean  $\pm$  standard deviation. The data of each group were analyzed by unpaired *t*-test, and the comparison of data among multiple groups were performed by one-way ANOVA and Tukey's post hoc test, *n* = 6, \**p* < 0.05 vs. the vector + CS group, #*p* < 0.05 vs. the vector + CS + vitamin E group.

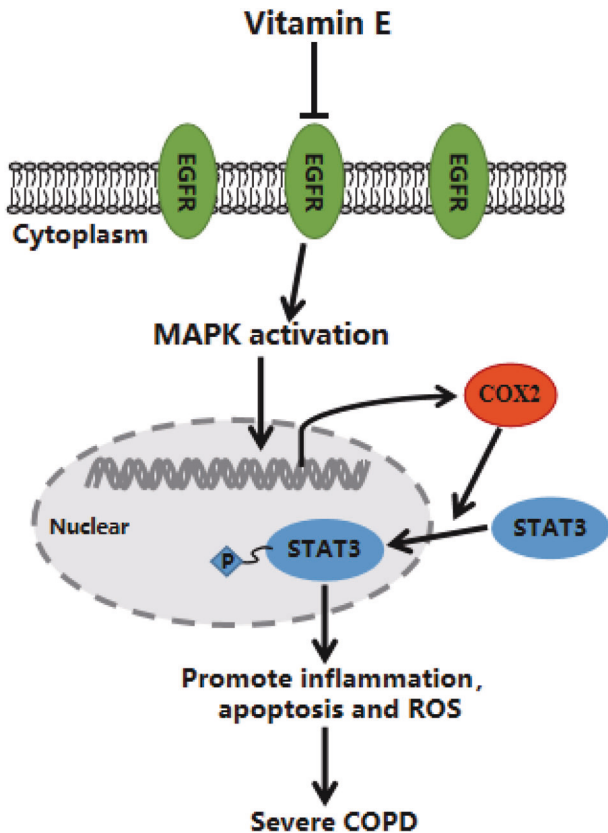


**Fig. 6 The mechanism graph of the regulatory function of Vitamin E in COPD.** Vitamin E relieves COPD by negatively regulating EGFR/MAPK pathway and inhibiting COX2-mediated translocation of phosphorylated STAT3 to the nucleus.

MAPK pathway, and COX2-mediated translocation of phosphorylated STAT3 to the nucleus. Given the progressiveness of COPD, understanding the roles of antioxidants in this disease could have a significant impact on the regulation of pathways contributing to the progression of COPD. The study provides an experimental basis for investigating the clinical use of vitamin E in the COPD patients, highlighting new prospects for COPD-targeted therapy.

**DATA AVAILABILITY**

The datasets generated/analyzed during the current study are available.

**REFERENCES**

- Hattab, Y., Alhassan, S., Balaan, M., Lega, M. & Singh, A. C. Chronic obstructive pulmonary disease. *Crit. Care Nurs. Q.* **39**, 124–130 (2016).
- Aldhahir, A. M. et al. Nutritional supplementation during pulmonary rehabilitation in COPD: a systematic review. *Chron. Respir. Dis.* **17**, 1479973120904953 (2020).
- Duffy, S. P. & Criner, G. J. Chronic obstructive pulmonary disease: evaluation and management. *Med. Clin. North. Am.* **103**, 453–461 (2019).
- Rovina, N., Koutsoukou, A. & Koulouris, N. G. Inflammation and immune response in COPD: where do we stand? *Mediators. Inflamm.* **2013**, 413735 (2013).
- Labaki, W. W. & Rosenberg, S. R. Chronic obstructive pulmonary disease. *Ann. Intern. Med.* **173**, ITC17–ITC32 (2020).
- Rabe, K. F. & Watz, H. Chronic obstructive pulmonary disease. *Lancet.* **389**, 1931–1940 (2017).
- MacNee, W. Pulmonary and systemic oxidant/antioxidant imbalance in chronic obstructive pulmonary disease. *Proc. Am. Thorac. Soc.* **2**, 50–60 (2005).
- MacNee, W. Oxidants/antioxidants and COPD. *Chest.* **117**, 303S–317S (2000).
- Peh, H. Y. et al. Vitamin E isoform gamma-tocotrienol protects against emphysema in cigarette smoke-induced COPD. *Free Radic. Biol. Med.* **110**, 332–344 (2017).
- Jiang, J. J., Chen, S. M., Li, H. Y., Xie, Q. M. & Yang, Y. M. TLR3 inhibitor and tyrosine kinase inhibitor attenuate cigarette smoke/poly I:C-induced airway inflammation and remodeling by the EGFR/TLR3/MAPK signaling pathway. *Eur. J. Pharmacol.* **890**, 173654 (2021).
- Cuschieri, J., Bulger, E., Biligren, J., Garcia, I. & Maier, R. V. Vitamin E inhibits endotoxin-mediated transport of phosphatases to lipid rafts. *Shock* **27**, 19–24 (2007).



12. Nag, S., Manna, K., Saha, M. & Das Saha, K. Tannic acid and vitamin E loaded PLGA nanoparticles ameliorate hepatic injury in a chronic alcoholic liver damage model via EGFR-AKT-STAT3 pathway. *Nanomedicine. (Lond)* **15**, 235–257 (2020).
13. Li, J. K. et al. IL-17 mediates inflammatory reactions via p38/c-Fos and JNK/c-Jun activation in an AP-1-dependent manner in human nucleus pulposus cells. *J. Transl. Med.* **14**, 77 (2016).
14. Morita, I. Distinct functions of COX-1 and COX-2. *Prostaglandins Other Lipid Mediat.* **68–69**, 165–175 (2002).
15. Cheng, J. et al. Contribution of alveolar type II cell-derived cyclooxygenase-2 to basal airway function, lung inflammation, and lung fibrosis. *FASEB J.* **30**, 160–173 (2016).
16. Yuan, J., Liu, R., Ma, Y., Zhang, Z. & Xie, Z. Curcumin attenuates airway inflammation and airway remodeling by inhibiting NF-kappaB signaling and COX-2 in cigarette smoke-induced COPD mice. *Inflammation* **41**, 1804–1814 (2018).
17. Kodama, Y. et al. Antioxidant nutrients in plasma of Japanese patients with chronic obstructive pulmonary disease, asthma-COPD overlap syndrome and bronchial asthma. *Clin. Respir. J.* **11**, 915–924 (2017).
18. Xantus, G. et al. The role of vitamin E acetate (VEA) and its derivatives in the vaping associated lung injury: systematic review of evidence. *Crit. Rev. Toxicol.* **51**, 15–23 (2021).
19. Agler, A. H. et al. Differential expression of vitamin E and selenium-responsive genes by disease severity in chronic obstructive pulmonary disease. *COPD.* **10**, 450–458 (2013).
20. Rodriguez-Rodriguez, E. et al. Antioxidant status in a group of institutionalised elderly people with chronic obstructive pulmonary disease. *Br. J. Nutr.* **115**, 1740–1747 (2016).
21. Tsiligianni, I. G. & van der Molen, T. A systematic review of the role of vitamin insufficiencies and supplementation in COPD. *Respir. Res.* **11**, 171 (2010).
22. Zhang, H. X. et al. HIF-1alpha promotes inflammatory response of chronic obstructive pulmonary disease by activating EGFR/PI3K/AKT pathway. *Eur. Rev. Med. Pharmacol. Sci.* **22**, 6077–6084 (2018).
23. Stolarczyk, M. et al. ADAM17 and EGFR regulate IL-6 receptor and amphiregulin mRNA expression and release in cigarette smoke-exposed primary bronchial epithelial cells from patients with chronic obstructive pulmonary disease (COPD). *Physiol. Rep.* **4**, e12878 (2016).
24. Sun, Y. et al. YKL-40 mediates airway remodeling in asthma via activating FAK and MAPK signaling pathway. *Cell. Cycle.* **19**, 1378–1390 (2020).
25. Eapen, M. S. et al. Apoptosis signal-regulating kinase 1 inhibition attenuates human airway smooth muscle growth and migration in chronic obstructive pulmonary disease. *Clin. Sci. (Lond)* **132**, 1615–1627 (2018).
26. Kuang, W. et al. Hepatocyte growth factor induces breast cancer cell invasion via the PI3K/Akt and p38 MAPK signaling pathways to up-regulate the expression of COX2. *Am. J. Transl. Res.* **9**, 3816–3826 (2017).
27. Tong, D. et al. Metformin inhibits castration-induced EMT in prostate cancer by repressing COX2/PGE2/STAT3 axis. *Cancer. Lett.* **389**, 23–32 (2017).
28. Wang, H. et al. STAT3 regulates the type I IFN-mediated antiviral response by interfering with the nuclear entry of STAT1. *Int. J. Mol. Sci.* **20**, 4870 (2019).
29. Guanizo, A. C., Fernando, C. D., Garama, D. J. & Gough, D. J. STAT3: a multifaceted oncoprotein. *Growth Factors* **36**, 1–14 (2018).
30. Rodrigues Brandao-Rangel, M. A. et al. Exercise inhibits the effects of smoke-induced COPD involving modulation of STAT3. *Oxid. Med. Cell Longev.* **2017**, 6572714 (2017).

## ACKNOWLEDGEMENTS

We would like to give our sincere appreciation to the reviewers for their helpful comments on this article.

## AUTHOR CONTRIBUTIONS

HZ, JG, LL, SZ, GY, PL, RL, and JL designed the study. LL, SZ, GY, PL, RL, and JL collated the data, carried out data analyses, and produced the initial draft of the paper. HZ, JG contributed to drafting the paper. All authors have read and approved the final submitted paper.

## FUNDING

This work is supported by Special Fund Project for the Central Government to Guide Local Science and Technology Development (YDZX20191400004736); Shanxi Province Key R&D Program (International Science and Technology Cooperation) Project (201903D421058).

## ETHICS APPROVAL

All animal experiments were approved by the Animal Care and Use Committee of The Second Hospital of Shanxi Medical University and in accordance with the guidance of National Institutes of Health. Great efforts were made to minimize the number of animals used in the experiments and their suffering.

## COMPETING INTERESTS

The authors declare no competing interests.

## ADDITIONAL INFORMATION

**Supplementary information** The online version contains supplementary material available at <https://doi.org/10.1038/s41374-021-00652-z>.

**Correspondence** and requests for materials should be addressed to Hui Zhao

**Reprints and permission information** is available at <http://www.nature.com/reprints>

**Publisher's note** Springer Nature remains neutral with regard to jurisdictional claims in published maps and institutional affiliations.



**Open Access** This article is licensed under a Creative Commons Attribution 4.0 International License, which permits use, sharing, adaptation, distribution and reproduction in any medium or format, as long as you give appropriate credit to the original author(s) and the source, provide a link to the Creative Commons license, and indicate if changes were made. The images or other third party material in this article are included in the article's Creative Commons license, unless indicated otherwise in a credit line to the material. If material is not included in the article's Creative Commons license and your intended use is not permitted by statutory regulation or exceeds the permitted use, you will need to obtain permission directly from the copyright holder. To view a copy of this license, visit <http://creativecommons.org/licenses/by/4.0/>.

© The Author(s), under exclusive licence to United States and Canadian Academy of Pathology 2021